Toughness Evaluation of a Shielded Metal Arc Carbon-Manganese Steel Welded Joint Subjected to Multiple Post Weld Heat Treatment

I. de S. Bott and J.C.G. Teixeira

(Submitted 29 January 1999; in revised form 16 July 1999)

This study was part of a program to investigate the influence of multiple post weld heat treatment (PWHT) on the fracture toughness and defect tolerance of a welded joint. The present work reports base metal data obtained for a quenched and tempered BS7191 Grade 450EM steel (0.10wt%C-1.08wt%Mn), weld metal data for a ferritic multipass weld obtained by shielded metal arc welding using an AWS E-9018M type electrode, and heat affected zone (HAZ) data obtained using a modified bead on groove technique for different PWHT conditions. The effect of the repeated heat treatment cycles on the mechanical properties was evaluated by hardness tests and toughness testing assessed by Charpy V-notch and crack tip opening displacement (CTOD) techniques. The characterization of the microstructure was undertaken utilizing optical and electron microscopy.

As fabrication codes for new equipment do not allow more than three PWHT cycles, the application of more cycles is only justifiable for old equipment when a fitness for purpose criterion is applied and these restrictions are not applicable. The results obtained are currently applied in repair work and revamps of pressure vessels and gas storage tanks.

Keywords C-Mn steel, embrittlement, post weld heat treatment, shielded metal arc welding, submerged arc welding

1. Introduction

1.1 Post Weld Heat Treatment

Fabrication codes for steel structures have become increasingly restrictive with respect to weld metal mechanical properties, where the current trend is to demand high impact resistance at low temperatures. Producers of weld consumables, in order to meet these specifications, have been in search of resources that will allow a rigid control of the high strength steel weld metal, such as the control of impurities; residual elements; for example, phosphorous, sulfur, and tin; and the increase of the volumetric fraction of acicular ferrite.

Though many fabrication codes offer guidance on the duration and temperature of post weld heat treatment (PWHT), these codes do not agree on the precise values of these parameters required to provide a suitable PWHT, which will reduce residual stresses to an acceptable level without compromising strength or toughness (Ref 1).

Repeated PWHT may, in some instances, result in a reduction in strength and degradation of toughness and defect tolerance of welded joints (Ref 2), a fact commonly overlooked in the commercial fabrication codes. A study of a welded joint was performed, taking into account the individual behavior of three distinct regions, heat affected zone (HAZ), weld metal, and base metal subjected to a number of PWHTcycles.

I. de S. Bott, Department of Materials Science and Metallurgy, Catholic University of Rio de Janeiro-PUC/Rio; R.Marquês de S. Vicente 235, Gávea CEP 22453-900, Rio de Janeiro, Brazil; **J.C.G. Teixeira,** PETROBAS-Research and Development Center, CENPES/DIPLOT/SEMEC, Rio de Janeiro, Brazil. Contact e-mail: bott@mail.rdc.puc-rio.br.

2. Experimental Procedures

Slow cooling in the range of 400 to 500 °C subsequent to PWHT may induce temper embrittlement in quenched and tempered steels and adversely affect their notch toughness. To determine whether embrittlement mechanisms can operate in these steels they were submitted to a multiple PWHT, consisting of 1, 2, 4, 7, and 20 cycles, each for 2 h duration at 590 °C according to AWS D1.1 (Ref 3). Post weld heat treatment was completed consisting of multiple cycles for 2 h duration at 590 °C, an average heating rate of 125 °C/h, and a cooling rate of 235 °C according to AWS D1.1 (Ref 3).

Vickers hardness, tensile, and Charpy V-notch testing were completed followed by microstructural characterization using optical and electron microscopy.

2.1 Materials

The base metal investigated was a quenched and tempered steel (BS7191 Grade 450EM) of 25 mm thickness, roller quenched from 900 °C, and tempered at 640 °C for 2 h. Table 1 gives the chemical composition. The welds, all weld metal test assemblies, were obtained using a preheating temperature of 100 °C, by a shielded metal arc multirun welding process in the flat position (approximately 20 passes, with temperature between passes of 150 °C) applying continuous current, positive to the electrode and utilizing a single bevel groove geometry; Fig. 1 shows the details. An AWS E-9018M type electrode of

3.25 mm diameter was used for the root pass, and 4.00 mm diameter was used for the filling passes. Table 1 gives the chemical analysis of the weld metal, and the chemical composition of the electrode wires is given in Table 2.

2.2 Welding Parameters

The weld metal investigated was obtained by shielded metal arc welding (SMAW) using an AWS E-9018M type electrode, at a nominal heat input of 2 kJ/mm, according to the schematic diagram shown in Fig. 1 and parameters described in Table 3.

The HAZ zone was obtained using a modified bead on groove technique. In order to guarantee the uniformity of the HAZ, welding was performed by submerged arc welding (SAW), keeping the same heat input (2 kJ/mm) as the SMAW welds, as shown in Table 3. The wires used in these welds, E8018D1 with flux LW880M, were not the object of this study because they were used solely to obtain the HAZ.

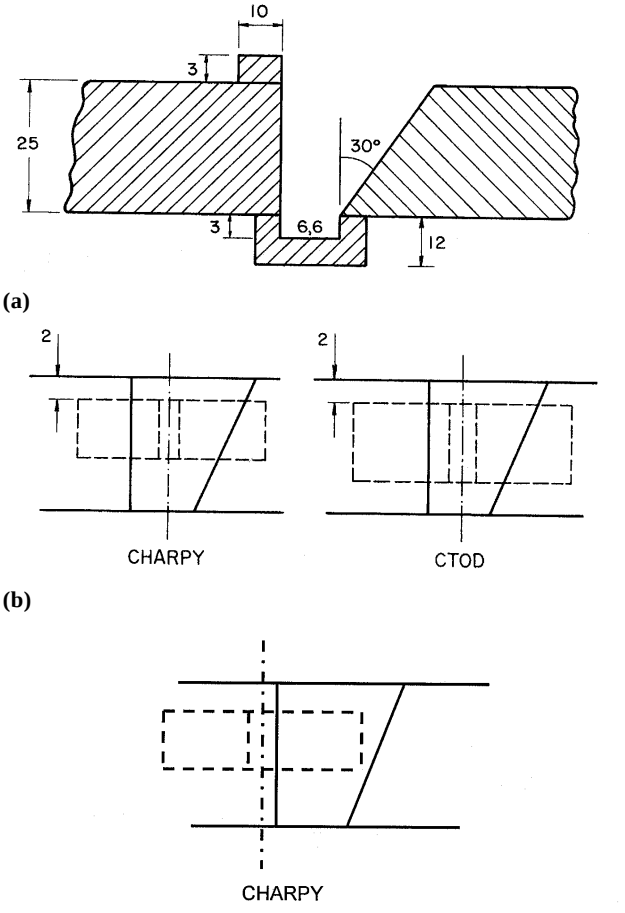

Fig. 1 (a) Schematic showing the weld joint for shielded metal arc welding. (b) Schematic of sampling, showing the notch position and depth from surface, for Charpy V-notch and crack tip opening displacement test pieces for the weld metal. (c) Schematic of sampling, showing the notch position and depth from surface, for Charpy V-notch for the heat affected zone. (All dimensions are in mm.)

3. Mechanical Testing

For all types of tests, five samples were tested for each heat treatment condition and testing temperature.

3.1 Sampling

Sampling of the base metal and weld metal was completed, as shown in the schematic diagrams of Fig. 2 and 3.

3.2 Hardness

Vickers hardness testing was undertaken with 30 g load for the base metal and HAZ, across the sample thickness and across the transverse section of the weld metal with a 5 g load. It should be mentioned that these measurements were intended to compare the influence of the PWHT on these two microstructures because they are different in nature.

3.3 Charpy V-Notch Testing

Base Metal. Toughness assessment by Charpy V-notch tests were performed at –30 and –40 °C and where the base metal was

Table 1 Chemical composition of the base metal and weld metal

	Composition, wt%	
Element	**Base metal**	**Weld metal**
C	0.10	0.06
Mn	1.08	1.12
Si	0.27	0.44
P	0.018	0.019
S	0.005	0.009
Cr	0.16	0.07
Cu	0.01	0.06
Mo	0.01	0.017
V	0.02	0.01
Ti	0.03	0.01
B	4 ppm	ND
Ni	0.03	1.22

ppm, parts per million; ND, no data

Table 2 Chemical composition of the electrode wires AWS E-9018M

	Composition, wt%	
Element	**3.25 mm diameter**	**4.0 mm diameter**
C	0.06	0.06
Mn	0.97	1.11
Si	0.51	0.38
P	0.018	0.019
S	0.013	0.007
Cr	0.045	0.040
Cu	ND	ND
Mo	0.22	0.26
V	0.01	0.01
Ti	ND	ND
B	ND	ND
Ni	1.69	1.56

ND, no data

sampled transversally to the rolling direction, as shown in Fig. 2.

Weld Metal. Figure 1(a) shows the weld joint geometry. In the case of the weld metal the specimens were sampled transversally to the joint (Fig. 3) at 2 mm depth from surface, as shown in Fig. 1(b).

Heat Affected Zone. The heat affected zone was sampled transversally to the joint and the notch positioned, as shown in Fig. 1(c).

3.4 Crack Tip Opening Displacement Testing

All crack tip opening displacement (CTOD) tests were complete at 0 and –10 °C, according to the ASTM E 1290 standard (Ref 4) and were interrupted at the maximum load, δ_m, CTOD. After CTOD testing, the test pieces were separated at liquid nitrogen temperature according to the procedure defined in the document API RP 2Z (Ref 5). In order to complete the microstructural analysis, these samples were transversely sectioned at the fatigue precrack tip.

Base Metal. The same sampling procedure for the base metal, as described for the previous testing procedure was repeated, as shown in Fig. 2.

Weld Metal. The weld metal specimens were sampled transversally to the joint at 2 mm depth from surface as shown in Fig. 1 and 3.

Heat Affected Zone. It is well established that the HAZ region of welded joints produced by multipass welds generally yields results, which are difficult to analyze due mainly to the scatter, observed in the CTOD values. This fact does not allow a correct evaluation of the joint performance because the final value obtained may correspond to different regions of the joint, such as the coarse grain heat affect zone (CGHAZ), fine grain heat affected zone (FGHAZ), or even weld metal.

To obtain the desired HAZ, a modified bead on groove technique was used (Ref 6). The technique applied consisted of machining a groove, on the steel plate surface, orientated at small angle ($\alpha = 2°$) to the rolling direction, as shown in Fig. 4(a). The angle, α, of the groove in relation to the rolling direction, was chosen to ensure that the fatigue precrack tip during propagation would necessarily pass through the CGHAZ in the central region of the test piece, as shown in Fig. 4(b). This arrangement permits a transverse section at the fatigue precrack tip of a CTOD test piece, of length, *L*, at the CGHAZ to

Table 3 Welding parameters

Parameter	Process	
	Shielded metal arc welding	Submerged arc welding
Heat input, kJ/mm	2.0	2
Polarity	CC^+	…
Current, A	160	550
Voltage, V	25	32.5
Speed, cm/min	13	54
Stick out, mm	…	35

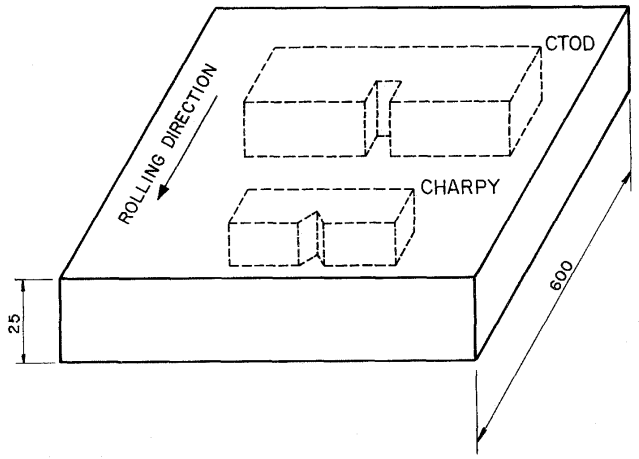

Fig. 2 Schematic of sampling for Charpy V-notch and crack tip opening displacement test pieces for the base metal. (All dimensions are in mm.)

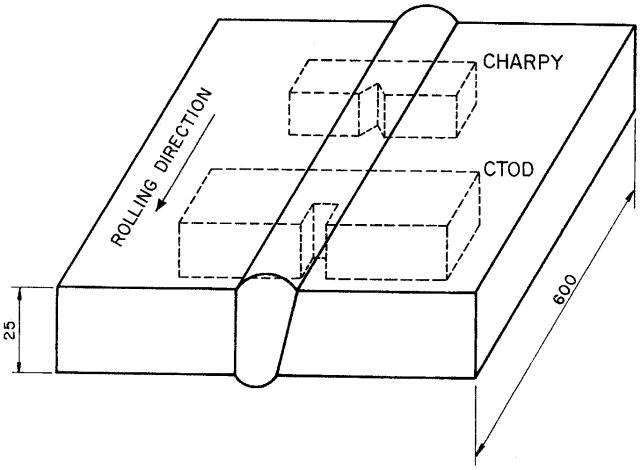

Fig. 3 Schematic of sampling for Charpy V-notch and crack tip opening displacement test pieces for the weld metal. (All dimensions are in mm.)

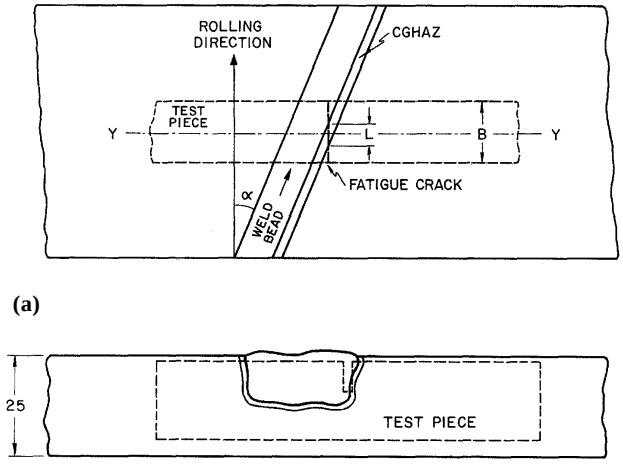

Fig. 4 (a) Schematic showing the weld joint for submerged arc welding. (b) Schematic of sampling, showing the notch position for crack tip displacement opening test pieces for heat affected zone, where *B* is test piece thickness and α is the angle between the rolling direction and the weld bead. (All dimensions are in mm.)

be intercepted. In the present study a 2 kJ/mm heat input weld was obtained by SAW to guarantee the section uniformity. The CGHAZ, the region of interest, was obtained through the first pass.

4. Metallographic Examination

Microstructural characterization by optical and scanning electron microscopy was completed for the base metal, weld metal, and HAZ. The terminology adopted followed that of the International Institute of Welding (IIW) (Ref 7).

5. Results

5.1 Hardness Testing

A reduction in strength and hardness (Fig. 5) can be expected because during PWHT the substructure responsible for the strengthening mechanism undergoes recovery (Ref 8). This is in agreement with classical behavior of a quenched and tempered martensitic alloy for which tempering decreases the strength and usually increases toughness (Ref 9). Some authors suggest that stress relief embrittlement characteristics are different from those of temper embrittlement (Ref 10), where the segregation of impurities such as phosphorous or tin can occur when the alloy is heated or cooled slowly through the range 375 to 575 °C. There are, however, different degrees of embrittlement, depending on the presence of specific alloying elements such as nickel, chromium, and molybdenum and the length of tempering time. A reduction of 4% in the average base metal hardness was observed, while the average weld metal hardness reduction was 13% after seven cycles at 590 °C. It should be mentioned, however, that there is a variation in hardness along the weld metal, being lower at the root than that obtained at the weld surface for the majority of situations.

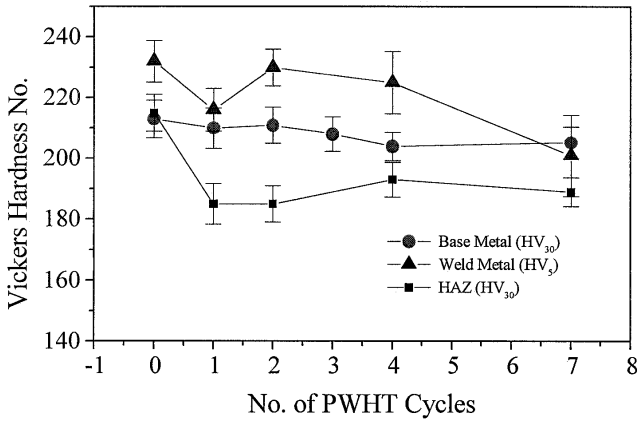

Fig. 5 Effect of the number of post weld heat treatment cycles at 590 °C for 2 h on hardness. The error bars represent the range of measured values.

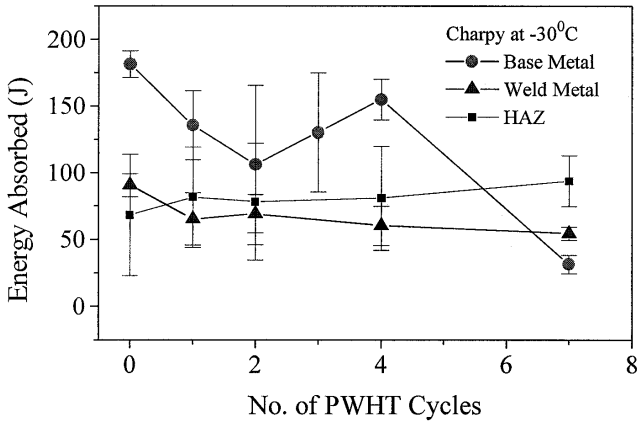

Fig. 6 Effect of the number of post weld heat treatment cycles at 590 °C for 2 h on Charpy testing at –30 °C. The error bars represent the range of measured values.

5.2 Charpy V-Notch Testing

For extended tempering, carbide transformations such as $Fe_3C \rightarrow M_7C_3$ can occur, and embrittlement by impurity segregation may also occur (Ref 11). Among several mechanisms proposed for embrittlement during PWHT (Ref 10), the common characteristic is the fact that trace elements have a less important role than for temper embrittlement, and brittle fracture occurs by transgranular cleavage. This mechanism, however, includes carbide coarsening effects, which in turn can also be considered to involve a temper embrittlement mechanism (Ref 12). It seems therefore, that the distinction between these two mechanisms is not very clear because both may involve carbide coarsening, which in turn can lead to impurity segregation.

Studies on welded joints tend to focus on a specific region, such as the weld metal or heat affected zone. From the Charpy results, Fig. 6 and 7, obtained at –30 and –40 °C, the base metal, rather than the weld metal or HAZ, shows a significant decrease in toughness after two and three PWHT cycles respectively. It can be observed from these figures that after the first cycle of PWHT there was a decrease in toughness for the base and weld metal, and a further increase in number of cycles did result in an even greater decrease for the base metal, indicating that the base metal is embrittled after seven cycles. The tendency observed up to four cycles remained for the weld metal and HAZ.

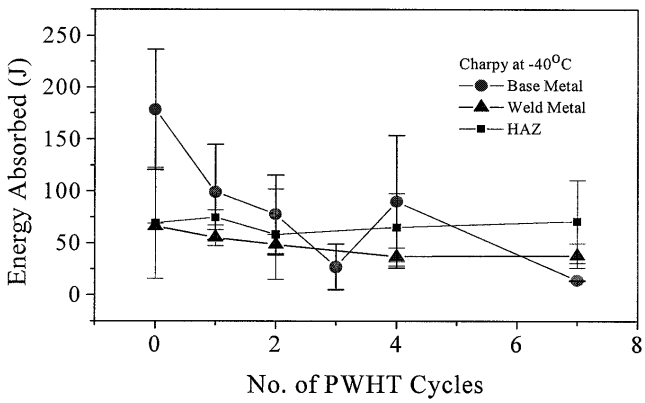

Fig. 7 Effect of the number of post weld heat treatment cycles at 590 °C for 2 h on Charpy testing at –40 °C. The error bars represent the range of measured values.

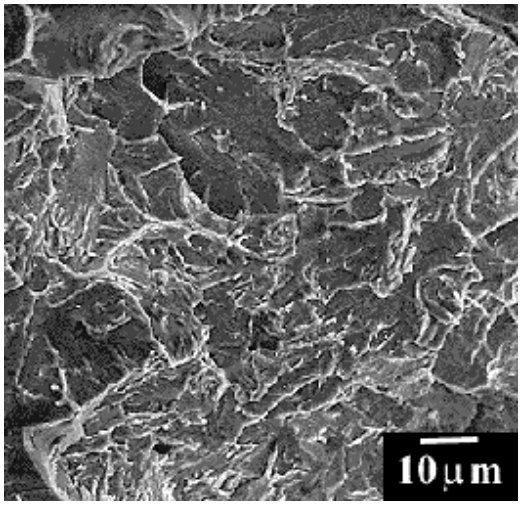

(a)

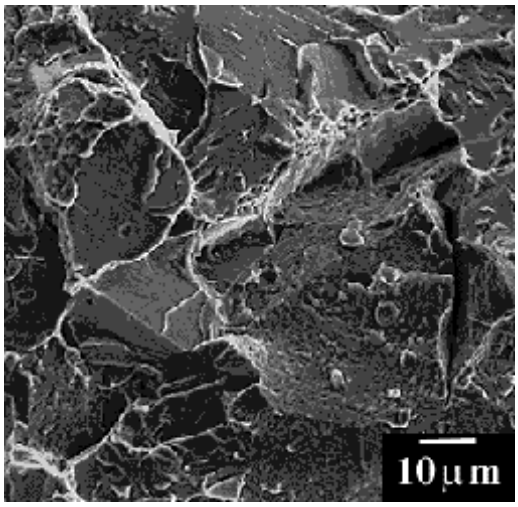

(b)

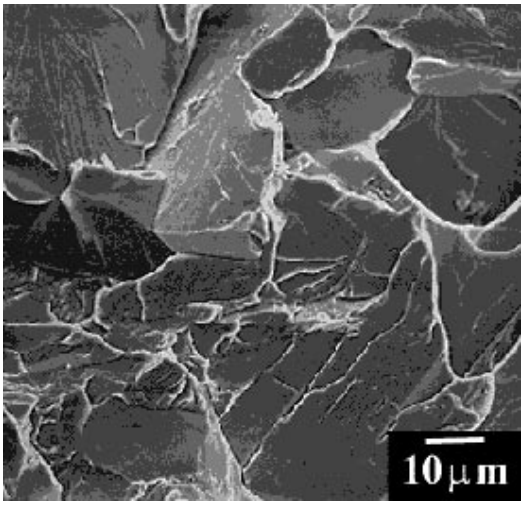

(c)

Fig. 8 Base metal fracture appearance at –30 °C. (a) As received condition. (b) After seven post welding heat treatment cycles at 590 °C for 2 h. (c) After 20 post weld heat treated cycles at 590 °C for 2 h

5.3 Fracture Analysis

The progressive embrittlement of the base metal is evident in Fig. 8. Metallographic examination showed extensive precipitation at the grain boundaries, as shown in Fig. 9(a). For Charpy testing at –30 °C, the fracture mode was initially quasi-cleavage changing to intergranular. This embrittlement was present after seven cycles of PWHT, as shown in Fig. 9(b). This was not the case for the weld metal, which showed a quasi-cleavage mode of fracture even at –196 °C for all cycles of PWHT, as shown in Fig. 10.

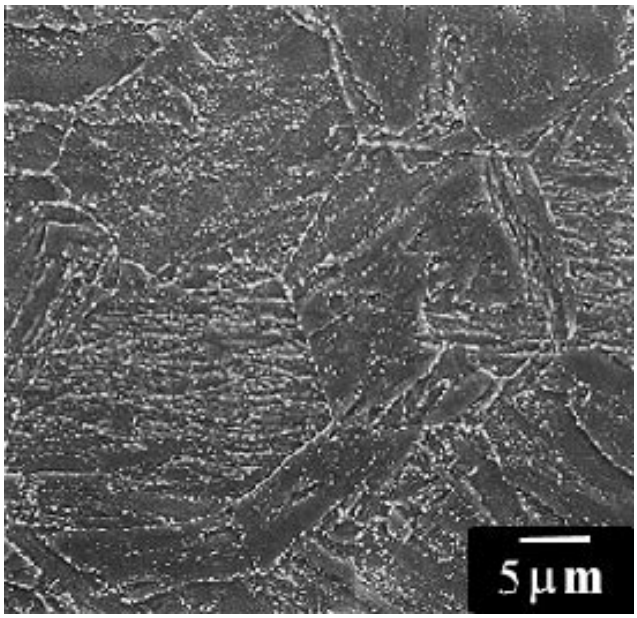

(a)

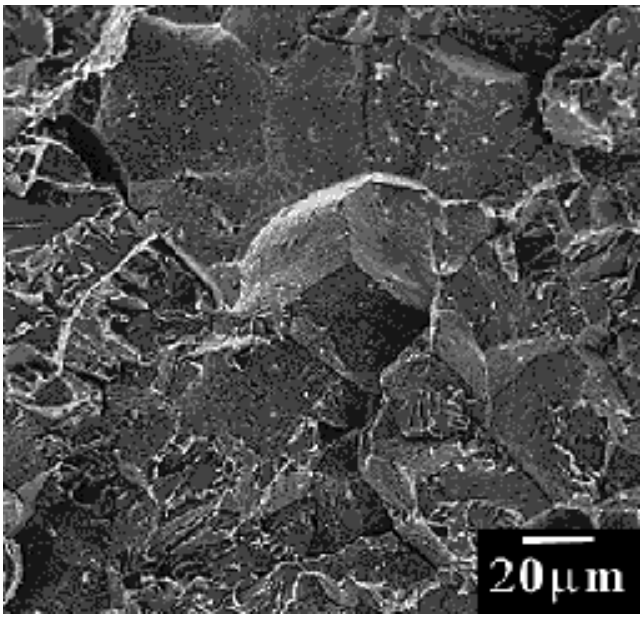

(b)

Fig. 9 Base metal after seven post weld heat treated cycles at 590 °C for 2 h. (a) Precipitation at grain boundaries, nital etch. (b) Fracture appearance at –196 °C

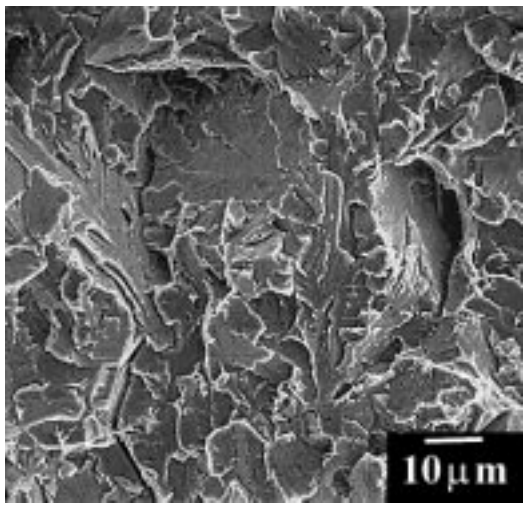

(a)

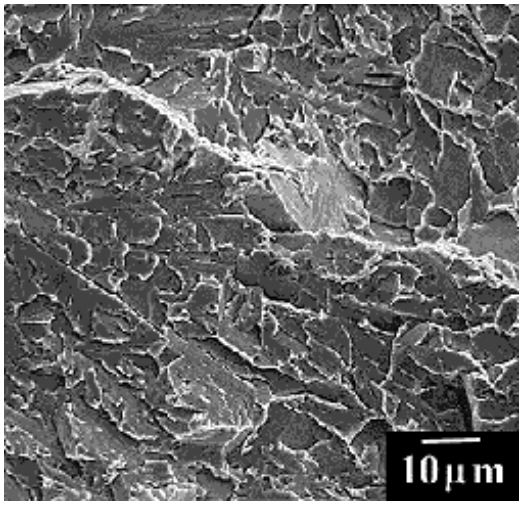

(b)

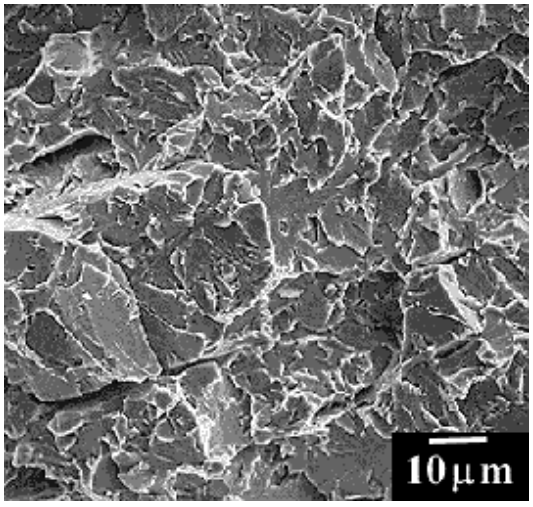

(c)

Fig. 10 Weld metal fracture appearance at –196 °C. (a) As received condition. (b) After seven post weld heat treated cycles at 590 °C for 2 h. (c) After 20 post weld heat treated cycles at 590 °C for 2 h

5.4 Crack Tip Opening Displacement Testing

The CTOD testing was carried out at 0 and –10 °C, as shown in Fig. 11 and 12 for the base metal, weld metal, and HAZ. For the latter it was necessary to simulate the process to minimize the scatter in the results because the major difficulty in analyzing HAZ fracture toughness results obtained for test specimens of multipass weld runs results from the complex crack propagation path, which typically passes through various distinctly different microstructural regions during the course of the test, leading to extensive scatter in the resulting data. It is important therefore, to apply HAZ simulation techniques capable of reproducing the microstructural characteristics representative of a real welded joint while controlling the geometrical distribution of the key microstructural zones in such a way to minimize the crack path complexity, reducing the scatter in test results. The technique adopted, modified bead on groove, showed that the lowest value of maximum load, δ_m, occurred after two cycles of PWHT for the base metal, followed by recovery after four cycles of PWHT. These results suggest that repeated PWHT may lead to a loss in toughness at a level significant for service performance. It should be observed, however, that it is the HAZ that will control the brittle fracture process.

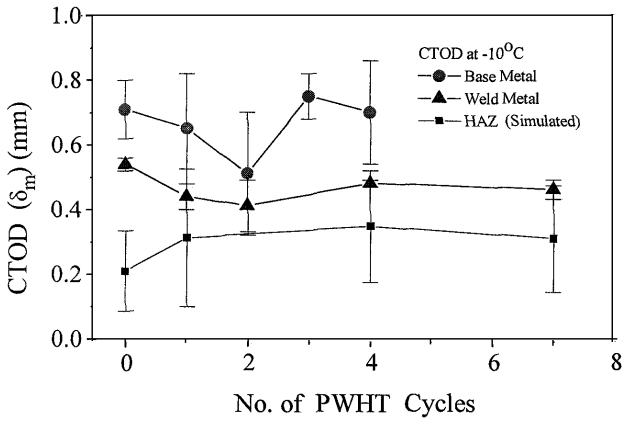

Fig. 11 Effect of the number of post weld heat treated cycles at 590 °C for 2 h on crack tip opening displacement testing at –10 °C. The error bars represent the range of measured values.

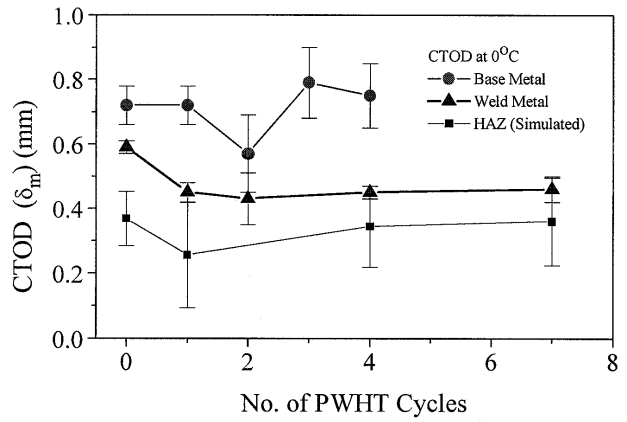

Fig. 12 Effect of the number of post weld heat treatment cycles at 590 °C for 2 h on crack tip opening displacement testing at 0 °C. The error bars represent the range of measured values.

6. Discussion

6.1 Base Metal

For extended tempering, carbide transformations can occur, and embrittlement by impurity rejection may occur (Ref 11). Among the several mechanisms proposed for embrittlement during stress relief (Ref 10), the common characteristic is the fact that trace elements have a less important role than is the case for temper embrittlement, and that brittle fracture occurs by transgranular cleavage. This mechanism however includes carbide coarsening which, in turn, can also be considered to contribute to the temper embrittlement mechanism (Ref 12).

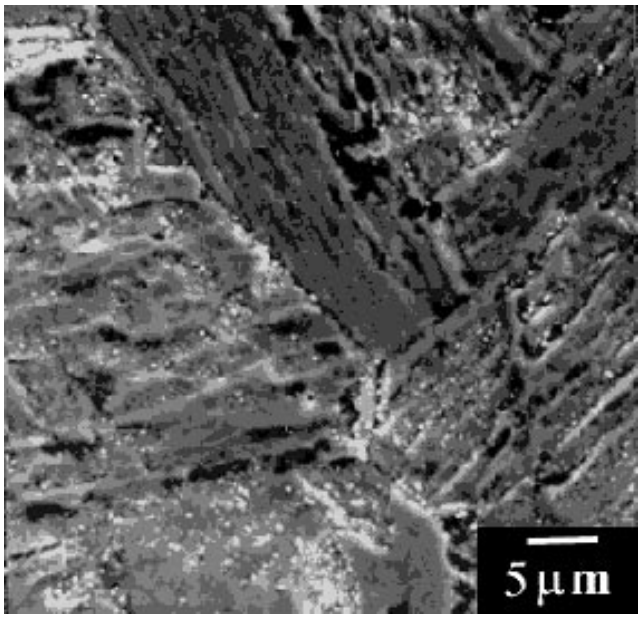

(a)

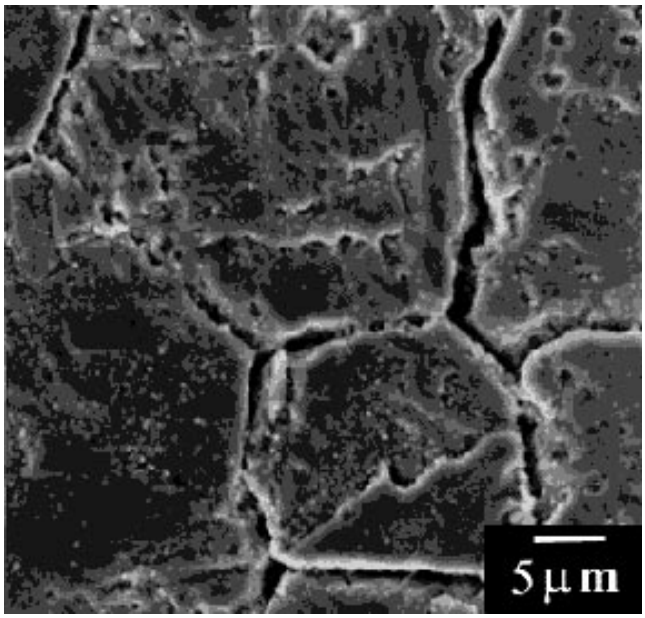

(b)

Fig. 13 (a) Base metal, in the as received condition, picral etch. (b) After two post weld heat treatment cycles at 590 °C for 2 h, picral etch

The Charpy impact test results revealed a minimum value at –30 °C after two cycles of heat treatment (Fig. 6) and at –40 °C after three cycles (Fig. 7). These results, which present a considerable scatter as indicated by the error bars, can be associated with the fact that the base metal temperature transition was within the range of the test temperature, which was –30 and –40 °C. This was emphasized by the fracture surface, which presented a mixed mode of fracture. Moreover, there was a maximum increase of ~23 °C in the transition temperature up to four cycles, indicating that embrittlement had occurred (Ref 13). It should be noted that the PWHT temperature was only 50 °C lower than the base metal tempering temperature itself. The fractographic analysis shows the progressive embrittlement of the base metal with increasing PWHT cycles, as shown in Fig. 8. This embrittlement can be associated with carbide coarsening (mainly Fe_3C as identified by transmission electron microscopy (TEM) and x-ray analysis, Ref 13) although not dissociated from temper embrittlement because a mixed cleavage and intergranular fracture was observed.

Metallographic examination, after etching with picral (Fig. 13), revealed more pronounced grain boundary definition for the sample subjected to two PWHT cycles (Fig. 13b) than for the specimen in the as-received condition (Fig. 13a). This tendency was clear after seven cycles of PWHT, although purely at a qualitative level. This indicates that phosphorus may have segregated to these boundaries. It should be remembered that this type of metallographic examination was one of the first methods to detect temper embrittlement by phosphorous (Ref 14). Currently, there are of course more sophisticated methods of surface analysis such as Auger electron spectroscopy (AES), which will be undertaken in a future phase of this study.

Therefore, in light of these metallographic results associated with toughness measurements, as shown in Fig. 11 and 12, which reveal a trough after two cycles of PWHT for CTOD testing at 0 and –10 °C, and for Charpy impact test at –30 °C (Fig. 6), there is some indication of embrittlement and recovery after the third cycle. Though microstructural evidence of changes is not clear at this level because heterogeneity was evident, carbide coarsening has however been detected (Ref 13). It can be suggested that repeated PWHT, that is, beyond four cycles, may lead to a loss of toughness at a level significant for service performance, according to Charpy V-notch results, but not according to CTOD results.

6.2 Weld Metal

In recent years attention has been drawn to the relationship between the microstructure and notch toughness of the weld metal, which is related to the volume fraction of each different constituent along the crack path (Ref 15). Therefore, all toughness results described in this article will be analyzed, taking into account the constituent volumetric fraction ahead of the notch and fatigue crack. Additionally, the terminology used for identification of the microstructural constituents will follow the guidelines of the IIW document (Ref 7).

Microstructural analysis showed that acicular ferrite at ~70 vol%, was the predominant constituent in the columnar region

for all conditions studied. The favorable influence of this constituent on toughness is primarily caused by the fine grain size (0.5 to 5.0 μm) and the fact that acicular ferrite is characterized by a favorable dislocation density and the absence of twin formation, which leads to plastic deformation rather than cleavage. Moreover the presence (in large numbers because of the small grain size) of high angle boundaries between adjacent regions impedes crack propagation (Ref 15).

In multipass welds the heat input of the subsequent passes causes tempering or PWHT effect on the earlier passes. This fact combined with the additional PWHT allows precipitates to grow and coalesce, and thus minimizes their effect (Ref 16).

The toughness values measured showed a small decrease (Fig. 6 and 7) after the first two cycles without further significant reduction for an extended number of cycles, the predominant refined region being along the notch, as shown in Table 4. In the case of CTOD tests (Table 5) the microstructural distribution along the fatigue crack showed that the fine grained region was predominant.

Table 4 Volume fraction (percent) of each microstructural region along the Charpy V-notch in the weld metal

Post weld heat treatment, cycles	Columnar region	Weld metal refined region	
		Fine grained	Coarse grained
0	20	42.5	37.5
1	10	71.5	18.5
2	25.5	52.5	22.5
4	22.50	60	17.5
7	17.50	60	22.5
20	15.7	56.7	20.5

Table 5 Volume fraction (percent) of each microstructural region along the fatigue crack (crack tip opening displacement) in the weld metal

Post weld heat treatment, cycles	Columnar region	Weld metal refined region	
		Fine grained	Coarse grained
0	21.25	51.25	27
1	15	53.75	31.25
2	32.5	45	22.5
4	25.9	50.1	24
7	22.5	62.5	15

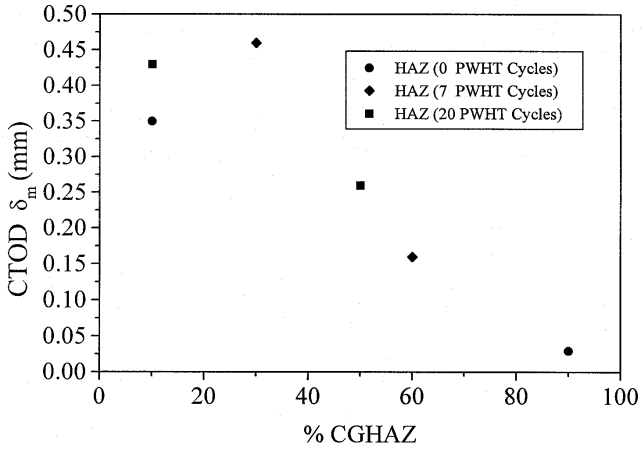

Fig. 14 Correlation between the percentage of coarse grained region of the heat affected zone region with crack tip opening displacement values

The fracture mode remained quasi-cleavage for all conditions studied (Fig. 10), confirming the absence of embrittlement in this alloy.

The toughness of multipass welds can be controlled by the toughness of high temperature reheated regions, rather than as-deposited weld metal. This may be because, for any given weld metal composition, the increased grain boundary area in reheated regions compared with columnar regions results in a smaller proportion of acicular ferrite and thus lower toughness (Ref 17). In general, the refined region confers upon the weld metal a better toughness performance than the columnar region (Ref 18). From metallographic analysis, some increase of the fine carbide precipitation (Ref 19) could be observed, which was favored by the PWHT temperature (590 °C). This in turn increases the probability of microcracks leading to toughness reduction (Ref 10). This is in agreement with the literature (Ref 16, 20), which reports that PWHT toughness reductions are bound to occur if the welding conditions and the PWHT cycle are such that the precipitation kinetics favor the development of finely dispersed coherent precipitates. In the case of multipass welds where the heat from subsequent passes provides a continuing autotempering effect, or in cases where the stress relieving cycle causes overaging of the precipitates, toughness reduction may, due to the growth, loss of coherence, and coalescence of the precipitates, lead to softening, as shown in Fig. 5.

6.3 Heat Affected Zone

In general it is expected that the HAZ would be the region in a post weld heated welded joint most susceptible to fail in service; its evaluation, however, can be complex. One difficulty in analyzing HAZ fracture toughness results obtained for specimens of multipass weld runs results from a complex crack propagation path, which typically passes through various microstructural regions during the test, leading to extensive scatter in the resulting data.

This is shown in the results obtained in this study because according to Charpy V-notch testing, the HAZ had the best toughness results of the three regions in the SMAW (Fig. 6 and 7) and the lowest in the SAW welds for CTOD testing (Fig. 11 and 12) after several thermal cycles. These results can be explained in terms of the different nature of the crack tip itself and the region sampled by the crack tip in each test. In the case of the Charpy V-notch testing, the crack tip is blunt (as compared with that of the CTOD), so the region sampled by the crack tip was not truly representative of the HAZ, the weld metal also having contributed, thereby, not allowing a conclusive result concerning the HAZ toughness.

In the case of the SAW welds for CTOD testing, not only was the test piece sampling designed in order to allow the fatigue crack tip to propagate within the HAZ coarse grained region, which is usually the weak link, but also the determination of the nature of the crack tip permits a more precise evaluation of this narrow region. As a result of this sampling, it can be seen in Fig. 14, that there was less scatter in

the CTOD results at –10 °C, and a correlation between the percentage of coarse grained region with CTOD values could be obtained, where a decrease of CTOD values correspond to an increase of the coarse grained region sampled by the fatigue crack tip.

The modified bead on groove technique with variable angle (Ref 6) allowed different percentages of the coarse grain heat affected zone (CGHAZ) to be intercepted by the fatigue precrack tip in CTOD test pieces. In this way it is possible to evaluate the effect of the different percentages of CGHAZ on the CTOD values obtained.

It is sometimes questioned whether the coarse grain region can be considered a local brittle zone (LBZ), or rather that it may be so classified (as an LBZ) only if a microstructural constituent of austenite and martensite (A-M) is formed (Ref 21-25).

The effect of PWHT up to 2 h at 550 °C on carbon-manganese alloys evaluated by CTOD testing has been reported as not being significant. In this work the extended number of cycles did not further decrease the toughness in agreement with the published data (Ref 26). However, a correlation of the CTOD values with the amount of coarse grained region sampled by the fatigue precrack tip permitted the determination of the lower bound toughness limit. Some authors suggest that this value does not depend on the LBZ length when it exceeds 2 or 3 mm (Ref 26-28). Conversely, Haze and Aihara (Ref 22) suggested a range of 2 to 4 mm for this same limit.

7. Conclusions

The following conclusions can be drawn:

- Whereas the evaluation of the effect of multiple PWHT on toughness showed that the base metal rather than the HAZ is affected, the HAZ toughness, though not affected by the PWHT, was shown by CTOD testing to behave as an LBZ at 0 and –10 °C.
- According to Charpy V-notch testing, the base metal has been affected by the PWHTs and presented a brittle mode of fracture after seven cycles. On these grounds it can be said that the base metal was affected and that this tendency tends to increase with increasing numbers of cycles.
- The HAZ, conversely, because of its relatively narrow width, does not show this tendency in Charpy V-notch testing because the sampling ahead of this region would have received contributions from other, different regions, such as the fusion line and weld metal. In order to measure HAZ toughness, a simulation of the HAZ, using the same heat input and joint geometry was utilized allowing the fatigue crack tip to sample the coarse grained region and revealing that this region behaved as a LBZ.
- It seems therefore that the evaluation of the joint performance by testing each region separately, has shown that the tendency for toughness deterioration of the HAZ is better evaluated by CTOD testing than Charpy-V notch testing. In the present case it is clear that the base metal is affected above four PWHT cycles. The HAZ, though not affected by the extended PWHT, behaved as an LBZ, as shown by CTOD testing. The weld metal Charpy V-notch toughness showed lesser reduction than the base metal after extended PWHT.

Acknowledgments

The authors wish to thank the following institutions, CNPq, CAPES, FAPERJ, and FINEP, for the financial support and CENPES/PETROBRÁS for technical support.

References

1. R.D. Stout, Postweld Heat Treatment of Pressure Vessel Steels, *WRC Bull.*, Vol 302, 1985, p 1-14
2. P.L. Threadgill and R.H. Leggatt, "Effects of Postweld Heat Treatment on Mechanical Properties and Residual Stress Levels of Submerged-Arc Welds in a C-Mn-Nb-Al Steel," Welding Research Report, No. 253, 1984, p 1-7
3. "Structural Welding Code—Steel," ANSI/AWS D1.1, American Welding Society, 1991
4. "Standard Test Method for Cracking Displacement Fracture Toughness Measurement," ASTM E 1290, 1989
5. "Recommended Practice for Pre-Production Qualification for Steel Plates for Offshore Structures," API RP2Z, 1987
6. C.R. Ouro, F.L. Bastian, and I. de S. Bott, Influence of Local Brittle Zone Size on the Heat Affected Zone Toughness of Structural Steel for Offshore Applications, *Conference Proceedings of the 4th Conference on Trends in Welding Research, International Trends in Welding Science and Technology*, H.B. Smartt, J.A. Johnson, and S.A. David, Ed., ASM International, 1996, p 519-525
7. "Revision 2, Guide to the Light Microscope Examination of Ferritic Steel Weld Metals," IIW Document, No. IX-1533-88, IXJ-123-87, June 1988
8. D.P. Fairchild and J.Y. Koo, The Effect of Post Weld Heat Treatment on the Microstructure and Toughness of Offshore Platform Steels, *Proc. of the 6th International Offshore Mechanics and Arctic Engineering Symposium* (Houston, Texas), Vol III, M.M. Salama, H.C. Rhee, and J.K. Koo, Ed., ASME, 1987, p 121-129
9. F.B. Pickering, *Physical Metallurgy and the Design of Steels. Materials Science Series*, Applied Science Publishers, Ltd., London, 1978
10. N. Shinoue, M. Sekizawa, and A.W. Pense, Long Time Stress Relief Effects, ASTM A 737, Grade B and C, Microalloyed Steels, *WRC Bull.*, Vol 322, 1987, p 33-41
11. I. de S. Bott, "The Role of Microstructure in Temper Embrittlement of Low Alloy Steel," Ph.D. Dissertation, Sheffield City Polytechnic, Sheffield, U.K., 1987
12. H. Erhart and H.J. Grabke, Equilibrium Segregation of Phosphorus at Grain Boundaries of Fe-P, Fe-C-P, Fe-Cr-P, and Fe-Cr-C-P Alloys, *Metal Sci.*, Vol 15, 1981, p 401-408
13. I. de S. Bott, A.C. Insfrán, C.R. Ouro, and J.C. Teixeira, The Effect of Multiple Post-Weld Heat Treatment (PWHT) on a Quenched and Tempered HSLA Steel, *Weld. World*, Vol 31 (No. 6), 1993, p 424-425
14. L.E. Samuels, *Optical Microscopy of Carbon Steels*, ASM International, 1992, p 378
15. S. Hoekstra, M.A. Munnig Schmid-van der Burg, and G. den Ouden, Microstructure and Notch Toughness of Ferritic Weld Metal, *Met. Constr.*, Vol 18 (No. 12), 1986, p 771-775
16. C.H. Entrekin, Jr., Effect of Stress Relief on Microalloyed Weld Metal Impact Properties, *Weld. Res. (Supplement of the Weld. J.)*, Aug 1983, p 197s-203s
17. P. Harrison and R. Farrar, Microstructural Development and Toughness of C-Mn and C-Mn-Ni Weld Metals Part 2, Toughness, *Met. Constr.*, Vol 19 (No. 8), 1987, p 447R-450R
18. G. Glover, J.T. MacGrath, M.J. Tinkler, and G.C. Wheatherly, The Influence of Cooling Rate and Composition on Weld Metal Microstructure in a C-Mn and HSLA Steel, *Weld. Res. (Supplement of Weld. J.)*, September 1987, p 267s-273s

19. H.R.M. Costa, I. de S. Ivani, and C.R. Ouro, Evaluation of the Effect of Multiple PWHT on the Microstructure and Mechanical Properties of a Ferritic Weld Metal, *IIW DOC IIA*, 1994, p 93-94
20. R.D. Thomas, Jr., Submerged Arc Welding of HSLA Steels, *Met. Prog.*, Vol 111 (No. 4), 1977, p 30-36
21. B.C. Kim, S. Lee, N.J. Kim, and D.Y. Lee, Microstructure and Local Brittle Zone Phenomena in High Strength Low Alloy Steel Welds, *Metal. Trans. A*, Vol 22, 1991, p 139-149
22. T. Haze and S. Aihara, Influence of Toughness on Size of LBZ on HAZ Toughness of HSLA Steels, *Proc. 7th Offshore Mechanics and Arctic Engineering Symposium* (Houston, TX), ASME, 1988, p 515-523
23. K. Ushino and Y. Ohno, A Study of Intercritical HAZ Embrittlement in HT50 for Offshore Structural Use, *Proc. 6th Offshore Mechanics and Arctic Engineering Symposium* (Houston, TX), ASME, 1987, p 159-165
24. Y. Kasamatsu, S. Takashima, and T. Hosoya, Influence of M-A Constituent on Toughness of HAZ of High Strength Weldable Structural Steels, *Tetsu-to-Hagane (J. Iron Steel Inst. Jpn.)*, Vol 65 (No. 81), 1979, p 222-231 (in Japanese)
25. H. Mimura and K. Aoki, "On the Toughness of Microstructure in Low Carbon Steels Subjected to Weld Thermal Cycles," IIW Document, OC. IX 629-61, 1980
26. D.J. Sparkles, N. Bailey, and T.G. Gooch, The Effect of PWHT on HAZ of Microalloyed C-Mn Submerged Arc Welds, *MS Technology*, 1990, p 1215-1225
27. K. Satoh and M. Toyoda, Evaluation of LBZ; HAZ Fracture Toughness Testing and Utilization of Toughness Data to Structural Integrity, *Proc. 7th Offshore Mechanics and Arctic Engineering Symposium* (Houston, TX), ASME, 1988, p 495-502
28. P.W. Baterson, E.S. Webster, and E.F. Walker, Assessment of HAZ Toughness Using Small Scale Tests, *Proc. 7th Offshore Mechanics and Arctic Engineering Symposium* (Houston, TX), ASME, 1988, p 257-265